

FUNDAMENTAL ANALYSIS OF LATERAL DISPLACEMENT ESTIMATION QUALITY IN ULTRASOUND ELASTOGRAPHY

Jianwen Luo¹ and Elisa E. Konofagou^{1,2}

Departments of ¹Biomedical Engineering and ²Radiology, Columbia University, New York, NY

ABSTRACT

Complementary to axial, lateral displacement and strain can provide important information on the biological soft tissues in all applications of elastography. In this paper, the effect of key parameters on the lateral displacement estimation was investigated, in simulations and phantom experiments. The performance of the lateral estimator was evaluated by measuring its associated bias, jitter and correlation coefficient of radio-frequency (RF) signals. Simulation results showed that the bias, jitter and correlation coefficient undergo periodic variations depending on the lateral displacement, with a period equal to the pitch (i.e., adjacent element distance). The performance of the lateral estimation was improved, when a smaller pitch, or a larger beamwidth, was used. The results of the phantom experiments were shown to be in good agreement with the simulation findings, including the periodic variation of the performance with lateral displacement, effect of pitch and beamwidth. In conclusion, smaller pitch and wider beamwidth were found to be the key in reducing the jitter error in the lateral displacement estimation.

Index Terms—Beamwidth, Bias, Elastography, Jitter, Lateral, Pitch

1. INTRODUCTION

Ultrasound elastography has been developed into an effective imaging method of inferring to the elastic properties of biological tissues [1]. This technique has been successfully applied to the diagnosis of breast lesions and is currently clinically used [2].

Typically, only the axial displacement and strain are estimated in ultrasound elastography. However, most biological tissues are nearly incompressible [3], i.e., the axial compression leads to expansion in the lateral and elevational directions. Estimation of the lateral displacement and strain may provide important additional information on the tissue mechanical properties.

Elastography has been shown capable of obtaining lateral displacements and strains. By taking advantage of the lateral estimation technique, lateral, shear strains and the Poisson's ratio have been shown capable of being estimated

[4, 5]. In cardiac applications, the axial / lateral estimation of myocardium were used to calculate the radial /circumferential, or principal strains, which are angle-independent and centroid-independent [6].

Previously reported efforts have concentrated on the performance analysis of the axial displacement and strain estimation using different parameters. However, there are only a few fundamental studies on the performance of the lateral displacement and strain estimation [4]. In particular, the effect of lateral displacement, pitch and beamwidth on the lateral displacement and strain estimation has not been thoroughly studied.

In this paper, we study the effect of different ultrasound imaging parameters (i.e., pitch and beamwidth) on the lateral displacement estimation under well-controlled simulation and experimental conditions, which only consider lateral rigid motion. In the simulations, a homogeneous phantom is displaced in the lateral direction without any axial displacement/strain or lateral strain. Phantom experiments using lateral rigid motion are also performed to validate the simulation findings.

2. METHODS

2.1 Simulation

The pre- and post-displaced RF signals were generated using a 2-D convolution-based linear scattering model [7]. The transducer PSF had a 60% -6 dB bandwidth, a 3.3 MHz center frequency and a -6 dB beamwidth varying between 1 and 6 mm. The sampling frequency of the RF signals was 20 MHz. The speed of sound in soft tissues was assumed to be equal to 1540 m/s.

The scattering function consisted of point scatterers uniformly distributed in a space of 100×50 mm² (width \times depth). The scatterer density was 12 scatterers/ wavelength. The 2-D PSF was convolved with the scattering function to obtain the pre-displaced RF signals. The scatterers were then moved in the lateral direction at a specific lateral displacement. The post-displaced RF signals were obtained from the convolution of the 2-D PSF and the post-displaced scattering function. Gaussian white noise was added to the RF signals simulated above. The sonographic signal-to-noise ratio (SNR_s) was set to be equal to 60 dB.

The algorithm developed by Konofagou and Ophir [4] was used to estimate the lateral displacements without the correlation weighting. The window size was equal to 3.85 mm with a 90% overlap. 1-D cosine interpolation was applied on the cross-correlation function to improve the estimation precision [8]. The average estimated lateral displacement was calculated in a region of interest (ROI) of $50 \times 50 \text{ mm}^2$ located at the center of the simulated phantom. The bias of the estimation was obtained by subtracting the simulated lateral motion from the average estimates, while the jitter was calculated to be equal to the standard deviation (SD) of the estimates. The mean and SD of the correlation coefficient were also calculated in the same ROI.

2.2 Experimental phantom

A polyacrylamide tissue-mimicking phantom was constructed. The phantom was placed in a water tank and subsequently immersed in degassed water. A 128-element linear-array transducer with center frequency of 7 MHz (model 10L5, Terason Ultrasound, Burlington, MA) was attached to a computer-controlled positioner (Velmex Inc., Bloomfield, NY) and placed below the water surface but without contact to the phantom. Efforts were made to align the lateral and axial axes of the transducer beam with the horizontal and vertical axes of the positioner, respectively. The pitch was approximately equal to 0.30 mm. A Terason 2000 ultrasound system (Teratech Corp., Burlington, MA) was used to drive the transducer. The RF signals were acquired at a sampling frequency of 30 MHz. Each RF frame consisted of 256 beams, twice the number of the elements using beamforming techniques.

The transducer was then moved by the positioner in the horizontal (or, approximately, lateral) direction at a step of 0.015 mm. Forty steps were performed to reach a maximum lateral motion of 0.6 mm. At each position, the RF signals were acquired at a sampling frequency of 30 MHz.

The axial and lateral displacements relative to the first RF frame were estimated [4]. A window size of 2.57 mm and a 90% overlap were used. Assuming a 2-D cosine function $f(x,y)$ near the peak of the cross-correlation function at (1,1), the 2-D subsample shifts of the peak were given by $\Delta x = -\theta_1 / \omega_1$ and $\Delta y = -\theta_2 / \omega_2$, respectively, where

$$\omega_1 = \cos^{-1}[(f(0,1) + f(2,1)) / 2f(1,1)],$$

$$\theta_1 = \tan^{-1}[(f(0,1) - f(2,1)) / (2f(1,1)\sin(\omega_1))],$$

$$\omega_2 = \cos^{-1}[(f(1,0) + f(1,2)) / 2f(1,1)], \text{ and}$$

$$\theta_2 = \tan^{-1}[(f(1,0) - f(1,2)) / (2f(1,1)\sin(\omega_2))].$$

In order to study the effect of the pitch on lateral displacement estimation, the acquired RF signals were decimated by a factor of 4 or 2 (i.e., from 256 to 128, or 64, beams) in the lateral direction. When 256 or 128 beams were used, the pitch was kept the same, i.e., 0.3 mm. When 64 beams were used, the pitch was increased from 0.3 to 0.6 mm. In order to compare the performance of different

beamwidths, three $5 \times 5 \text{ mm}^2$ ROI's were selected, one near the focal zone and the other two 6.5 mm away from the focal zone. The centers of the ROI's were at depths of 2.15, 2.8 and 3.45 cm, respectively. For ROI's I, II and III, the beamwidth was equal to 0.9, 1.3 and 1.7 mm, respectively, as measured using the backscattered signals from a 5-0 (1.0 metric) braided thread (Ethicon Inc., Somerville, NJ).

3. RESULTS

3.1 Simulation results

Figure 1 shows the effect of the magnitude of the applied lateral displacement on the lateral displacement estimation at a fixed pitch (0.625 mm) and beamwidth (2 mm). Figure 2 compares the estimator performance at different pitches at a fixed beamwidth (2 mm). Figure 3 depicts the beamwidth effect on the lateral displacement estimation at a fixed pitch (0.625 mm).

Figure 1(a) shows that the estimation algorithm performs reliably over the entire range of the lateral displacement (i.e., 0-3 pitches). A linear relationship between the applied and estimated displacements is shown ($r > 0.999$). As shown in Figs. 2(b)-(d), all three performance indices undergo a periodic variation, with the period equal to the pitch. When the displacement is equal to half-integer pitch multiples (e.g., 0, 0.5, 1, 1.5 or 2 pitches), the bias is the lowest and nearly zero. The jitter reaches a minimum at integer pitch multiples (e.g., 0, 1 or 2 pitches) and maximum at odd half-integer pitch multiples (e.g., 0.5, 1.5 or 2.5 pitches), respectively. On the other hand, the correlation coefficient is maximum at integer pitch multiples and minimum at odd half-integer pitch multiples, respectively.

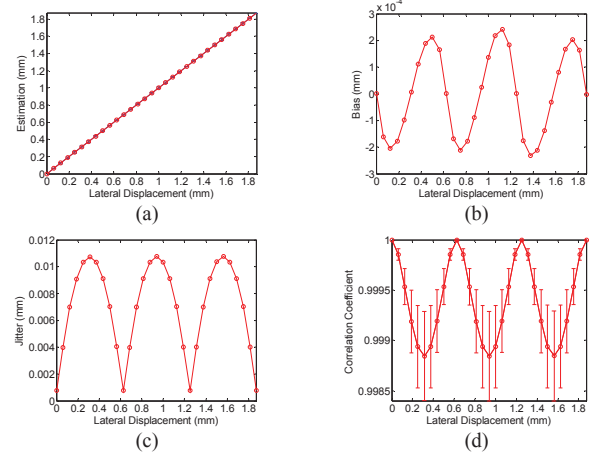


Figure 1. Effect of lateral displacement in the simulation study. (a) the estimated displacement, (b) bias, (c) jitter and (d) correlation coefficient as a function of the applied lateral displacement.

As shown in Figs. 2(b)-(d), the estimator performance improves as the pitch decreases, i.e., the jitter and bias drop while the correlation coefficient increases. The 3-D plot of the jitter against the pitch and lateral displacement in Fig. 2(a) shows the same variation as Fig. 2(c).

As evident in Figs. 3(b)-(d), both the bias and jitter decrease while the correlation coefficient increases when

the beamwidth increases. The 3-D plot of the jitter against the beamwidth and lateral displacement in Fig. 3(a) also shows lower jitter at larger beamwidths.

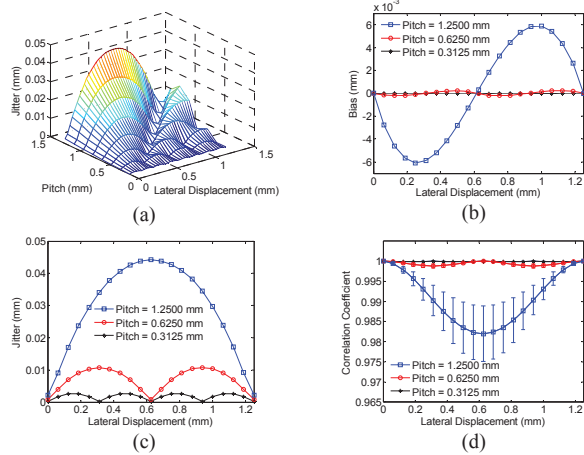


Figure 2. Effect of pitch in simulation. (a) jitter varied with pitch and lateral displacement, (b) bias, (c) jitter and (d) correlation coefficient.

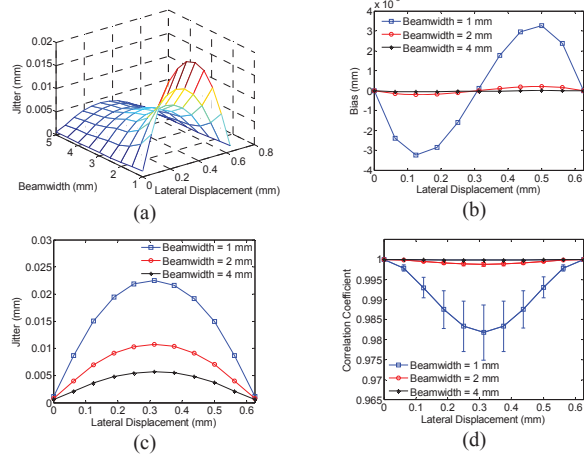


Figure 3. Effect of beamwidth in simulation. (a) jitter varied with beamwidth and lateral displacement, (b) bias, (c) jitter and (d) correlation coefficient.

3.2 Phantom results

When 256, or 128, beams are used, a linear relationship between the true and estimated lateral displacements is shown in Fig. 4(a) ($r > 0.999$). By using 64 beams, however, the displacement is underestimated, or overestimated, when the displacement is between 0 and 0.3 mm, or between 0.3 and 0.6 mm, respectively, due to the presence of estimation bias.

Using a total beam number of 64, the bias is minimum when the displacement is 0, 0.5 or 1 pitch multiples (i.e., 0, 0.3 or 0.6 mm) (Fig. 4(b)), i.e., when the original RF signals are used or adjacent beams contribute to the interpolated sub-beams equally. The bias for the 0.30-mm pitch (i.e., 256 or 128 beams) is very small (< 0.005 mm) and does not clearly exhibit a periodic variation with the lateral displacement. For both 0.30- and 0.60-mm pitches, the jitter is the lowest (or, the highest), and the correlation coefficient is the highest (or, the lowest), when the displacement is

equal to integer pitch multiples (or, at odd half-integer pitch multiples) (Figs. 4(c) and (d)). As is evident in Figs. 4(b)-(d), a pitch of 0.3 mm could result in significantly lower bias and jitter and higher correlation coefficient, demonstrating the importance of a smaller pitch in the lateral displacement estimation. The maximum jitter is approximately equal to $10 \mu\text{m}$ when a pitch of 0.3 mm is used.

Figure 4(d) also shows that the correlation coefficient is slightly higher at increased beam density from 128 to 256 beams. When 256 beams are used, the jitter is also slightly lower, except at lateral displacements around 0.15 or 0.45 mm (Fig. 4(c)). The bias remains similar in both cases (Fig. 4(b)). The variation period is also the same in both cases because the pitch is the same (0.3 mm).

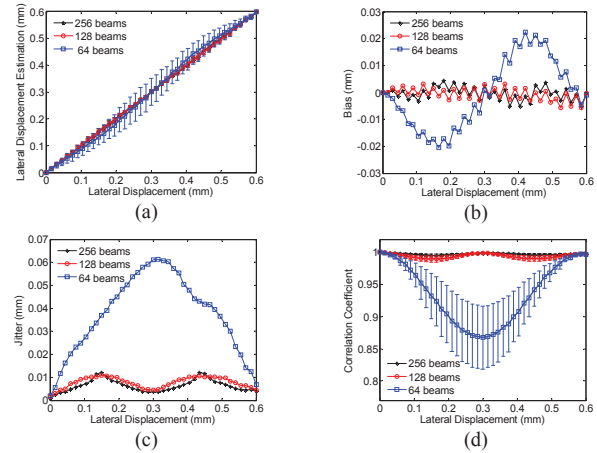


Figure 4. Effect of lateral displacements and pitch in phantom experiment. (a) the estimated displacement, (b) bias, (c) jitter and (d) correlation coefficient.

Figure 5 compares the performance of the estimation in ROI's I, II and III. The same periodic variation can be observed in the jitter and correlation coefficient of three ROI's. In addition, the jitter is the lowest in region III and highest in region I, except for displacements between 0.5 and 0.6 mm, while the correlation coefficient is the highest in region III and the lowest in region I. These results can be explained by the largest beamwidth in region III (1.7 mm) and smallest beamwidth in region I (0.9 mm). Although similar across the three ROI's, the bias appears slightly lower in region III than in regions I and II (Fig. 5(a)), because of the wider beamwidth, similar to the simulation results (Fig. 3). These experimental results in different regions and beamwidths are thus in good agreement with the simulation results.

4. DISCUSSION

In this study, lateral rigid motion was modeled in simulation in order to evaluate the performance of a lateral displacement estimator. In the phantom experiments, the phantom did not undergo any deformation while the transducer was moved in the lateral direction. In both simulation and experimental results, the correlation

coefficients between the pre- and post-displaced RF signals were much higher than in the presence of strains, because only lateral rigid motion was considered.

The results of the simulation and phantom experiments clearly demonstrate a periodic variation in the performance of the lateral displacement estimation (i.e., bias, jitter and correlation coefficient) at different lateral displacements, with the period equal to the pitch.

As shown in Figs. 2 and 3, in order to reduce the bias and jitter of the lateral displacement estimation, a smaller pitch and a larger beamwidth are preferred. At smaller pitch, the transducer provides more beams, which are the reliable data instead of the post-interpolation, reconstructed beams. However, a small pitch may complicate the design of the transducer. At larger beamwidths, the adjacent beams share more ultrasound scatterers and the RF signals of these beams are more statistically dependent. Therefore, it may be more accurate to interpolate the RF signals between adjacent beams. As a result, increasing the beamwidth reduces the jitter and bias. However, the trade-off is the reduced lateral resolution, so it will be dictated by the specific application.

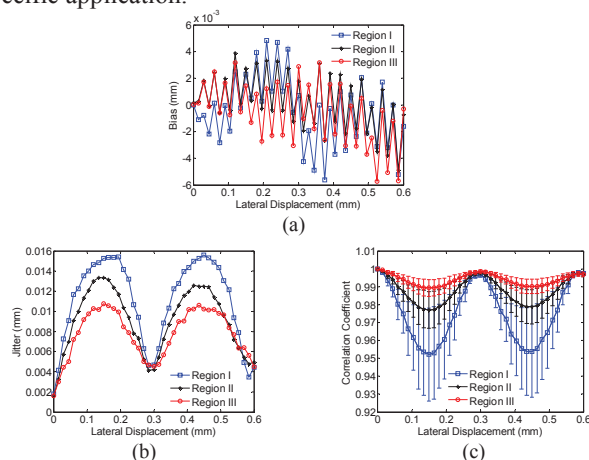


Figure 5. Effect of beamwidth in phantom experiment. (a) bias, (b) jitter and (c) correlation coefficient.

When the tissue undergoes a fixed lateral strain, according to this study, the performance of the lateral displacement estimation periodically varies with the beam position. When the lateral strains vary spatially, the bias of lateral displacement estimation has a similar variation with the beam position, which may result in the “zebra” artifact [8] in the lateral strain images.

The results of the lateral displacement estimation in this study may also be extended to the elevational displacement estimation and other estimation algorithms such as sum absolute difference (SAD), sum squared difference (SSD) as well as methods using 2-D kernels.

6. CONCLUSION

Simulation and phantom experiments were performed to investigate the effect of various parameters on lateral displacement estimation in ultrasound elastography. A

lateral rigid motion configuration was applied in order to eliminate the effect of axial displacement / strain and lateral strain on the lateral displacement estimation. The estimator performance as indicated by the bias, jitter and correlation coefficient shows a periodic variation with lateral displacement with a period equal to the pitch. Due to the periodic variation, a larger lateral displacement might be preferred to improve the SNR of the estimation. The performance was found to improve with a decreased pitch and/or an increased beamwidth. A smaller pitch was preferred at the same beam overlap, because the effect of pitch on lateral displacement estimation appeared to be larger than that of the beamwidth. In summary, smaller pitch and wider beamwidth are required in order to reduce the jitter error of the lateral displacement estimation. Our recent study also showed that the use of cubic spline, instead of linear interpolation, increases the correlation coefficient, and decreases the jitter, with the trade-off of slightly increased bias [9].

7. ACKNOWLEDGMENT

This study was supported in part by the American Heart Association (SDG0435444T), National Institutes of Health (R01EB006042) and the Wallace H. Coulter foundation. We wish to thank Caroline Maleke, M.S., and Yao-Sheng Tung, M.S., from our laboratory, for preparing the phantom used in this study.

REFERENCES

- [1] J. Ophir, I. Céspedes, H. Ponnekanti, Y. Yazdi, and X. Li, "Elastography: A quantitative method for imaging the elasticity of biological tissues," *Ultrason. Imaging*, vol. 13, pp. 111-134, 1991.
- [2] A. Itoh, E. Ueno, E. Tohno, H. Kamma, H. Takahashi, T. Shiina, M. Yamakawa, and T. Matsumura, "Breast disease: Clinical application of US elastography for diagnosis," *Radiology*, vol. 239, pp. 341-350, 2006.
- [3] Y. C. Fung, *Biomechanics: Mechanical Properties of Living Tissues*, 2nd ed. New York, NY: Springer-Verlag, 1993.
- [4] E. Konofagou and J. Ophir, "A new elastographic method for estimation and imaging of lateral displacements, lateral strains, corrected axial strains and Poisson's ratios in tissues," *Ultrasound Med. Biol.*, vol. 24, pp. 1183-1199, 1998.
- [5] E. E. Konofagou, T. Harrigan, and J. Ophir, "Shear strain estimation and lesion mobility assessment in elastography," *Ultrasonics*, vol. 38, pp. 400-404, 2000.
- [6] I. K. Zervantonakis, S. D. Fung-Kee-Fung, W.-N. Lee, and E. E. Konofagou, "A novel, view-independent method for strain mapping in myocardial elastography: eliminating angle and centroid dependence," *Phys. Med. Biol.*, vol. 52, pp. 4063-4080, 2007.
- [7] R. L. Maurice and M. Bertrand, "Speckle-motion artifact under tissue shearing," *IEEE Trans. Ultrason. Ferroelectr. Freq. Control*, vol. 46, pp. 584-594, 1999.
- [8] I. Céspedes, Y. Huang, J. Ophir, and S. Spratt, "Methods for estimation of subsample time delays of digitized echo signals," *Ultrason. Imaging*, vol. 17 (2), pp. 142-171, 1995.
- [9] J. Luo and E. E. Konofagou, "Fundamental analysis of key parameters for precise lateral displacement estimation in elastography with experimental validation," *Ultrasound Med. Biol.*, 2009, in press.